

The holographic deconfined QGP phase diagram and entropy with an anomalous flow in a magnetic field background

Jiali Deng¹ and Sheng-Qin Feng^{1,2,*}

¹*College of Science, China Three Gorges University, Yichang 443002, China*

²*Key Laboratory of Quark and Lepton Physics (MOE) and Institute of Particle Physics,
Central China Normal University, Wuhan 430079, China*

(Dated: September 22, 2021)

Abstract

It is well known that in the early stage of relativistic heavy ion non-central collision, there will be a large magnetic field eB , and the confinement-deconfinement phase transition also occurs in the early stage of collision. The strong magnetic field will produce novel anomalous transport phenomenon, which corresponds to the chiral magnetic effect and causes anomalous flow. This paper introduces the concept of anomalous flow, aiming at the phase transition characteristics of RHIC and LHC energy region: in the range of magnetic field and small chemical potential. The deconfinement phase transition in a strongly coupled chiral plasma in the presence of magnetic field and axial charge imbalance is studied by analyzing the characteristics of the effective string tension with different temperatures, chemical potentials, and magnetic fields in this paper. It is found that the anomalous flow would modify the characteristic of deconfinement phase transition. The characteristics of reporting inverse magnetic catalysis for the deconfinement transition with anomalous flow is in qualitative agreement with lattice QCD findings. A sharp peak of the heavy-quarkonium entropy around the deconfinement transition can be realized in our model, which is also consistent with the lattice QCD result.

* fengsq@ctgu.edu.cn

I. INTRODUCTION

The dissociation of charmonium and bottomonium bound states has been proposed as a signal for the formation of a hot and deconfined quark-gluon plasma by Matsui and Satz [1]. Quarkonium bound states such as charmonium $c\bar{c}$ and bottomonium $b\bar{b}$ will dissociate because of color screening and thereby exhibit a suppression relative to the confined phase in a deconfined QGP. Because of the importance of the problem, $c\bar{c}$ and $b\bar{b}$ dissociation in QGP have been a focus of many recent studies [2].

Some analyses of the $q\bar{q}$ dissociation of phenomenon are based on the study of the quark-antiquark static potential taken from lattice QCD [3]. However, the produced quarkonium bound state is not static, but has a velocity $v = \tanh(\eta)$ with respect to the medium in relativistic heavy ion collisions. If the relative velocity of quarkonium exceeds a typical thermal velocity, it can be considered that the quarkonium suppression is stronger than the thermal dissociation in a static heat bath [4, 5]. In the presence of an external magnetic field, the problem of quarkonium dissociation in a parity-violating chiral plasma with a finite chiral (axial) charge density was investigated [6]. This environment of quark gluon plasma (QGP) is a approximately chiral one which can be created in relativistic heavy-ion collisions. When two relativistic heavy ions collide with a non-zero impact parameter, a strong magnetic field with a magnitude of the order of [7–14] $eB \sim m_\pi^2$ (m_π is the pion mass), is produced in the direction of the angular momentum of the collision.

The chirality imbalance should have experimental consequences in such a strong magnetic field. If the chirality is non-zero, the quark spins are locked either parallel or anti-parallel to the magnetic field direction, depending on the quark charge. This would lead to a charge separation in the final state, and an electromagnetic current is generated along the direction of the magnetic field [10–14]. Anomaly-induced effects in a QGP medium, which is called chiral magnetic effect (CME) [15–18], has attracted much attentions [19, 20].

An quantitative analysis of the anomalous flow v_{anom} was investigated [6] experienced by a charmonium for a large class of chiral plasma with a gravity dual in the presence of magnetic field and axial charge imbalance. This type of plasma carries anomalous flow introduced by the chiral anomaly and manifests novel transport phenomena. The generation of vector current \mathbf{j}_v is along an external magnetic field \mathbf{B} , and those anomalous effects change hydrodynamics of chiral fluids [21]. The frame in which the energy density of such fluid is

at rest, is called the Landau frame. But the entropy density in the frame is not at rest and is moving in the direction of chiral magnetic current $\vec{j}_{\text{CME}} = C_A \mu_A \vec{B}$ [6]:

$$\vec{s}_{\text{anom}} = s v_{\text{anom}} \vec{B}, v_{\text{anom}} = -\frac{C_A \mu_A \mu}{\varepsilon + p}, C_A = \frac{N_C}{2\pi^2}, \quad (1)$$

where v_{anom} is the anomalous flow velocity, and $s, \varepsilon, \mu, \mu_A, p$ denote the entropy density, energy density, vector chemical potential, axial chemical potential and pressure respectively, and the coefficient C_A is fixed by the chiral anomaly. For small $|v_{\text{anom}}| \ll 1$, Ref.[6] investigated the charmonium dissociation in a strong coupled chiral plasma with a magnetic field at linear order in v_{anom} . Anomalous contributions to the heavy quark drag force were studied for a holographic chiral fluids [22].

It is well known that QCD is in the deconfinement phase at a high temperature and density, while the confinement phase is at a relative low temperature and density. The probe of the phase structure of QCD is an important and challenging assignment. It is generally realized that there is a phase transition between the two phases. How to study phase diagrams $T - \mu$ in the plane is a rather hard job because the QCD coupling constant becomes very large near the phase change region, and the traditional perturbation QCD method can not be used. For a long time, the lattice QCD method is regarded as the only credible way to study the problem. Although lattice QCD works well for zero density, but it has the sign problem when taking finite density into account. However, the most interesting region in the QCD phase diagram is at a finite density. The most concerned subjects, such as relativistic heavy-ion collisions and compact stars in astrophysics, are all related to a finite density of QCD.

This situation was greatly improved with the advent of the AdS/CFT correspondence to intrigue interest again in finding a string description of the strong interactions. Its evolving theory called AdS/QCD uses a five-dimensional effective description and attempts to fit QCD as much as possible. The effective string tension was used to discuss the thermal phase transition characteristics of a static $q\bar{q}$ pair [23]. And then it was extended to discuss the thermal phase transition of the moving quarkonium [24]. Ref. [24, 25] utilized effective string tension to study deconfined phase transition with a background magnetic field.

In recent years, some publications [26–32] studied holographically the effect of a background magnetic field on the chiral condensate and deconfinement transition. Specifically, more advanced phenomenological bottom-up holographic QCD models, which arrived at

the solution of the gravity equations, have been established that emerge inverse magnetic catalysis. Sensible $2 + 1$ dimensions gravity solutions manifesting inverse magnetic catalysis have been found in [26–28], and Refs. [30, 31] manifested the possibility of inverse catalysis in the $3 + 1$ dimensions deconfinement phase transition.

It is a standard procedure to study a confinement-deconfinement phase transition by checking the different configurations of a quark and antiquark in AdS/QCD [33–35]. The heavy quark pair can be regarded as a probe to detect whether the system is in a confinement or deconfinement phase. In this paper, we consider the chiral anomaly caused by a strong magnetic field, and to further study deconfinement phase transition. The dependencies of anomalous flow induced by a strong magnetic field on the phase transition characteristics of confinement and deconfinement are studied in this paper. Our study provides further insights on the anomalous flow felt by heavy probes of the chiral plasma in relativistic heavy-ion collisions.

In this work, we will use quarkonium to probe such an anomalous chiral fluid. Based on the discussion of anomalous flow, the deconfinement phase transition is further discussed. The paper is organized as follows. In Sec.II, we introduce our holographic set-up. In Sec. III, we introduce the effective string tension with the anomalous flow to study deconfined phase diagram. The entropy with chiral fluids is computed in Sec. IV. We make a short discussion and conclusion in Sec. V.

II. THE SET-UP

By dealing with a nonzero axial chemical potential, which taken as a manifestation of the chiral imbalance, and with a homogeneous external magnetic field B , we begin to use the 5-dimensional asymptotic AdS₅ bulk metric which is corresponding to the dense strongly coupled plasma of $N = 4$ SYM theory. Such metric can be defined by solving the bulk Einstein- Maxwell- Chern-Simons equations. In the presence of the anomalous flow, we will study the situation when the v_{anom} is small. Consequently, the bulk metric, at leading order in v_{anom} , can be obtained by solving the linearized bulk equation of motion around AdS Reissner-Nordstrom (RN) black-brane solution, see Refs. [6, 36–38] for details. The

resulting metric, in the Landau frame of the fluid, is as follows:

$$ds^2 = \frac{h(z)}{z^2}(-f(z)dt^2 + d\vec{x}^2 - 2v_{\text{anom}}Q(z)dx_3dt) + \frac{2h(z)v_{\text{anom}}Q(z)}{z^2f(z)}dzdx_3 + \frac{h(z)}{z^2f(z)}dz^2, \quad (2)$$

where $h(z) = e^{cz^2/2}$ is a warp factor, which illustrates the characteristics of the soft wall model, and the deformation parameter $c = 0.9\text{GeV}^2$ depicts the deviation from conformality [39–41]. For $N = 4$ SYM theory with a nonzero chemical potential and with a weak homogeneous external magnetic field B , some functions such as $f(z)$ and $Q(z)$ [6, 42] can be given as

$$f(z) = 1 - Mz^4 + q^2z^6, \quad (3)$$

$$Q(z) = 2\pi^2T^2z^2 - \pi^4T^4z^4 + 2(1 - \pi^4T^4z^4)\log\left(\frac{1}{1 + \pi^2T^2z^2}\right) + O(\mu^2/T^2), \quad (4)$$

and black hole parameters q and M , which could be related to chemical potential and temperature T [6, 22, 37]

$$q = \frac{\mu\pi^2T^2}{2\sqrt{3}} \left[\sqrt{\frac{8\mu^2}{3\pi^2T^2} + 1} + 1 \right]^2, \quad (5)$$

$$M = \frac{\pi^4T^4}{16} \left[\sqrt{\frac{8\mu^2}{3\pi^2T^2} + 1} + 1 \right]^3 \left[3\sqrt{\frac{8\mu^2}{3\pi^2T^2} + 1} - 1 \right]. \quad (6)$$

By considering a $q\bar{q}$ dipole moving through a thermal plasma at the velocity $v = \tanh(\eta)$, we choose the plasma is at rest, and the dipole is moving with a constant rapidity η along the x_3 direction (see Fig. 1 for a schematic view). It is convenient to take the gravity background Eq.(2) in the frame that the dipole is at rest while energy density of the QGP medium is moving with rapidity $-\eta$ in the x_3 direction. In our discussion, the $q\bar{q}$ dipole now is at rest and feels a hot plasma wind

$$dt = dt' \cosh(\eta) - dx'_3 \sinh(\eta), \quad (7)$$

$$dx_3 = -dt' \sinh(\eta) + dx'_3 \cosh(\eta). \quad (8)$$

After dropping the prime, we get the metric

$$\begin{aligned} ds^2 = & \frac{h(z)}{z^2} [(-f(z) \cosh^2(\eta) + \sinh^2(\eta) + v_{\text{anom}}Q(z) \sinh(2\eta))dt^2 + dx_1^2 \\ & + \frac{dz^2}{f(z)} + (-f(z) \sinh^2(\eta) + \cosh^2(\eta) + v_{\text{anom}}Q(z) \sinh(2\eta))dx_3^2 \\ & + (-\frac{2v_{\text{anom}}Q(z)}{f(z)} \sinh(\eta)dt dz + \frac{2v_{\text{anom}}Q(z)}{f(z)} \cosh(\eta)dx_3 dz)] + dx_2^2 \\ & + (f(z) \sinh(2\eta) - \sinh(2\eta) - 2v_{\text{anom}}Q(z)(\cosh^2(\eta) - \sinh^2(\eta)))dt dx_3. \end{aligned} \quad (9)$$

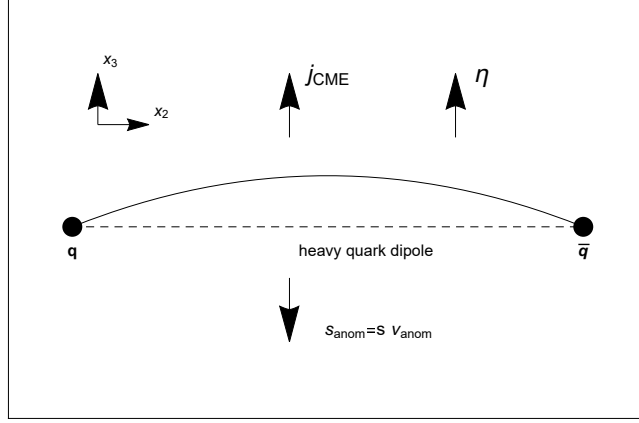


FIG. 1. A schematically picture of the heavy-quark dipole configuration and the corresponding string world-sheet (projected into $x_2 - x_3$ plane) in the holographic set-up considered in this paper. The chiral magnetic current is along x_3 -direction and the “dipole” is placed along x_2 -direction. The entropy flow s_{anom} is opposite to the chiral magnetic current. Without the anomalous flow v_{anom} , the string profile is constant along x_3 -direction (dashed curve between the heavy-quark dipole). However, the anomalous flow will stretch the string profile along x_3 direction (solid curve between the heavy-quark dipole).

The Nambu-Goto action of the world sheet in the Minkowski metric is given as

$$S_{\text{NG}} = -\frac{1}{2\pi\alpha'} \int d^2\xi \sqrt{-\det g_{ab}}, \quad (10)$$

where g_{ab} is the induced metric on the world sheet and $\frac{1}{2\pi\alpha'}$ is the string tension, and

$$g_{ab} = g_{MN} \partial_a X^M \partial_b X^N, \quad (11)$$

where X^M and g_{MN} are the coordinates and the metric of the AdS space. By using the static gauge $\xi^0 = t$, $\xi^1 = x_2$. We give the Nambu-Goto action as

$$S_{\text{NG}} = -\frac{1}{2\pi\alpha'T} \int_{-L/2}^{L/2} dx_2 \sqrt{g_2(z) + g_1(z) \left(\frac{dz}{dx_2}\right)^2 + f(z) \left(\frac{h(z)}{z^2} \frac{dx_3}{dx_2}\right)^2 + g_3(z) \frac{dx_3}{dx_2} \frac{dz}{dx_2}}, \quad (12)$$

where

$$g_2(z) = \frac{h^2(z)}{z^4} (f(z) \cosh^2(\eta) - \sinh^2(\eta) - v_{\text{anom}} Q(z) \sinh(2\eta)), \quad (13)$$

$$g_1(z) = \frac{g_2(z)}{f(z)}, g_3(z) = 2v_{\text{anom}} Q(z) \cosh(\eta) \left(\frac{h(z)}{z^2}\right)^2. \quad (14)$$

The separating distances of $q\bar{q}$ pair is given as

$$L = 2 \int_0^{z_0} \left[\frac{g_2(z)}{g_1(z)} \left(\frac{g_2(z)}{g_2(z_0)} - 1 \right) \right]^{-1/2} dz. \quad (15)$$

Since the anomalous contributions is governed by the magnitude of the anomalous flow v_{anom} , let us state our study by estimating the size of v_{anom} in relativistic heavy-ion collisions. By studying the dependence on charge e , C_A in Eq.(1), we get:

$$C_A = \frac{C_{\text{EM}} e^2}{2\pi^2}, \quad (16)$$

if considering the case that only u , d quark, we get the contributions to the CME current with $N_f = 2$, $C_{\text{EM}} = 5/9$. The equations of state of a massless ideal quark-gluon gas are given as

$$p = \frac{g_{\text{QGP}} \pi^2}{90} T^4, \quad \varepsilon = 3p, \quad (17)$$

where $g_{\text{QGP}} = g_G + \frac{7}{8}g_Q$ is the number of degrees of freedom with gluon $g_G = (N_C^2 - 1)N_s$ and quark $g_Q = 2N_C N_s N_f$, $N_C = 3$, $N_f = 2$ and $N_s = 2$ are the numbers of colors, flavors and spin states, respectively. Therefore, we have

$$v_{\text{anom}} \approx -0.003 \left(\frac{eB}{T^2} \right) \left(\frac{\mu_V \mu_A}{T^2} \right). \quad (18)$$

It is kindly reminded that the characteristic of eB and μ^2 is of order T^2 in Eq. (18), therefore one can find v_{anom} is numerically small. Extremely high magnetic fields $eB \approx 2m_\pi^2 (\sim 0.04 \text{ GeV}^2)$ [7, 14] can be produced in noncentral Au - Au collisions for top collision energies $\sqrt{s_{\text{NN}}} = 200 \text{ GeV}$ in the Relativistic Heavy Ion Collider (RHIC) at Brookhaven National Lab (BNL). these magnetic fields even though decay quickly, they only decay to a tenth of the original value for a time scale of order of the inverse of the saturation scale at RHIC [13, 43–46], hence they may affect the properties of the particles produced during the collision. Even larger field, of order $eB \approx 15m_\pi^2 (\sim 0.3 \text{ GeV}^2)$, can be produced for the energy reachable at the Large Hadron Collider (LHC) at CERN, $\sqrt{s_{\text{NN}}} = 4.5 \text{ TeV}$, for the Pb-Pb collisions [43, 44]. Those numbers can be even bigger from event by event fluctuations[10, 11]. This would cause a significant v_{anom} , but satisfies $|v_{\text{anom}}| \ll 1$. Therefore it would be interesting to regard situation that eB is large and study if anomaly induced flow would bring to a new mechanism for quarkonium suppression at early time in relativistic heavy-ion collisions. This suggests that our results based on small v_{anom} expansion is applicable to many situations in relativistic heavy-ion collisions.

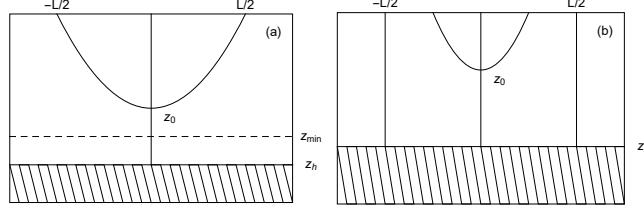


FIG. 2. (a) displays the characteristics of a U-shape open string, which links the $q\bar{q}$ with the confinement phase, and (b) displays two straight strings, which arrives the position of horizon at large separating distances in the deconfinement phase.

III. EFFECTIVE STRING TENSION AND PHASE DIAGRAM IN THE PRESENCE OF ANOMALOUS FLOW

A fundamental string connects the $q\bar{q}$ as shown in Fig. 2(a), and a U-shape open string connects the $q\bar{q}$ in the confinement phase. The deconfinement phase of the broken U-shape string is shown in Fig. 2(b).

Fig. 2(a) shows a U-shape open string links the $q\bar{q}$ in the confinement phase. A dynamic wall z_{\min} exists at a low temperature, and the U-shape string can not exceed the dynamic wall with increasing the separating distances of the $q\bar{q}$ pair as shown in the situation of $T < T_C$ (T_C phase transition temperature). z_0 is the lowest position of the U-shape string. When the temperature enhances to a certain value (T_C) and the value of horizon distance z_h gets small, the system will experience a confinement - deconfinement phase transition. Fig. 2(b) shows the broken U-shape string, in which the broken string changes into two straight strings at large separating distances, and reach the position of the horizon. In the situation, a large black hole appears, and the dynamic wall disappears. The critical temperature (T_C) can be interpreted as a confinement- deconfinement phase transition temperature. The U-shape string still exists in the deconfinement phase if the separating distances L of $q\bar{q}$ pair is small.

By considering the anomalous flow, the effective string tension is given as follows:

$$\sigma(z) = \sqrt{g_2(z)} = \frac{h(z)}{z^2} \sqrt{f(z) \cosh^2(\eta) - \sinh^2(\eta) - v_{\text{anom}} Q(z) \sinh(2\eta)}, \quad (19)$$

Eq. (19) gives the formula of effective string tension $\sigma(z)$ of the moving quarkonium with the anomalous flow. It is found that the effective string tension $\sigma(z)$ is a function of temperature, chemical potential, moving rapidity and anomalous flow v_{anom} . For fixed values of the chemical potential $\mu = 0.1$ GeV, and rapidity $\eta = 0.3$ and temperature $T = 0.1$ GeV,

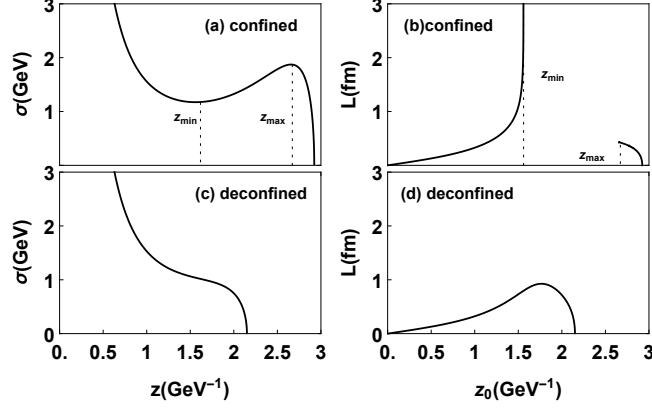


FIG. 3. The effective string tension corresponds to the confined situation (a) and deconfined phase (c), respectively. The dependencies of interquark distances L on the lowest position z_0 of the U-shape string are exhibited in the confined (b) and deconfined phase(d), respectively.

the dependence of the effective string tension $\sigma(z)$ on the fifth holographic coordinate z in the confined situation is given in Fig. 3(a). The effective string tension $\sigma(z)$ reaches a minimum when $z = z_{\min}$, and $\sigma(z)$ reaches the maximum value when $z = z_{\max}$. The dependence of distance L on z_0 in the confined situation is computed from the Eq.(15) as shown in Fig. 3(b). The distance increases monotonically from $L(z_0) = 0$ to $L(z_{\min}) \rightarrow \infty$ at $0 \leq z_0 \leq z_{\min}$. But at $z_{\max} \leq z_0 \leq z_h$ region, L monotonically decreases from a finite value $L(z_{\max})$ to $L(z_h) = 0$.

with the increase of temperature T ($T < T_C$), the two points z_{\min} and z_{\max} get more and more close along the z direction. When the temperature T increases to a certain value such as a phase transition temperature T_C , the two points z_{\min} and z_{\max} coincide at $z_{\min} = z_{\max} = z_m$. The effective string tension $\sigma(z)$ can be evaluated in Fig. 3(c) by taking $\mu = 0.1\text{GeV}$ and $T = 0.14\text{GeV}$. Fig. 3(d) shows that when $T > T_C$, $L(z)$ never exceeds the value $L(z_m)$ at $0 \leq z_0 \leq z_h$. For $L > L(z_m)$, two strings extend from the boundary $z_0 = 0$ to the black hole horizon $z_0 = z_h$ as shown in Fig. 2(b). The quark-antiquark pair splits into two quarks.

From Eq. (5), we can derive the dependence of phase transition temperature T_C on q_C as follows:

$$T_C = Aq_C^{1/2} + \frac{B}{q_C^{1/2}}, \quad (20)$$

where $A = \frac{\sqrt{27\sqrt{3}}}{3\pi\sqrt{6\mu}}$ and $B = -\frac{4\mu^3}{3\sqrt{3}}A$. By expanding phase transition temperature T_C to the leading order in v_{anom} , we can give

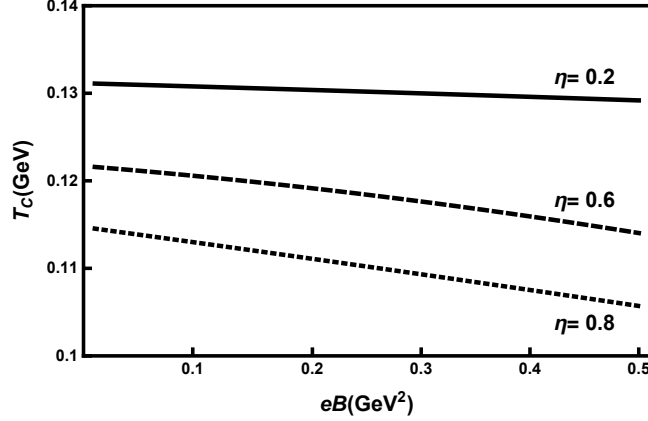


FIG. 4. The dependence of thermal AdS-black hole phase transition critical temperature T_C on magnetic field eB at different moving rapidity. Here $\mu = 0.01\text{GeV}$ is considered.

$$T_C = T_{C0} + v_{\text{anom}} \left(\frac{A}{2q_{C0}^{1/2}} - \frac{B}{2q_{C0}^{3/2}} \right) q_{C1}, \quad (21)$$

where

$$T_{C0} = T_C(q_{C0}), \quad (22)$$

$$T_C = T_{C0} + v_{\text{anom}} T_{C1}. \quad (23)$$

The temperature change caused by anomalous flow is

$$T_{C1} = \left(\frac{A}{2q_{C0}^{1/2}} - \frac{B}{2q_{C0}^{3/2}} \right) q_{C1}, \quad (24)$$

the detailed derivation process of q_C , q_{C0} and q_{C1} are given in the appendix of the paper.

In the RHIC and LHC energy regions, it is generally believed that the phase transition will occur at high temperature and low chemical potential. We also know that in the early stage of relativistic heavy ion non-central collision, there will be a large magnetic field eB , and the confinement-deconfinement phase transition also occurs in the early stage of collision. The strong magnetic field will produce novel anomalous transport phenomenon, which corresponds to the chiral magnetic effect and causes anomalous flow. This paper introduces the concept of anomalous flow, aiming at the phase transition characteristics of RHIC and LHC energy region: in the range of magnetic field (less than 0.3 GeV^2) and small chemical potential.

The dependence of phase transition critical temperature T_C on eB at different moving rapidity η are shown in Fig.4. In particular, T_C decreases with the increase of the magnetic

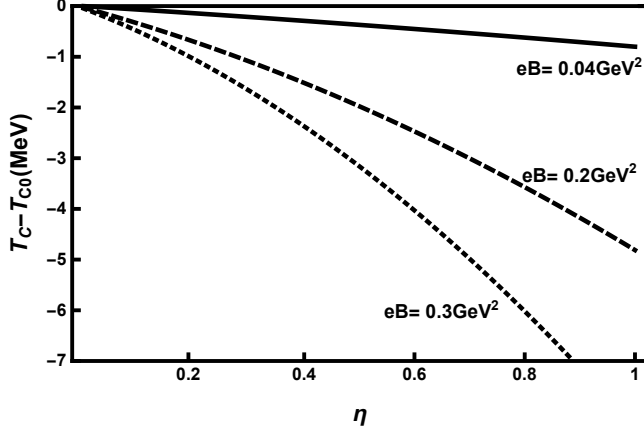


FIG. 5. The dependence of the change of phase transition temperature caused by anomalous flow on moving rapidity η at different magnetic field eB .

field. Since these thermal AdS and black hole phases in the usual language of gauge-gravity duality are dual to the confinement and deconfinement phases in the dual boundary theory, accordingly, our result in Fig.4 predicts inverse magnetic catalysis for the dual confinement-deconfinement transition. The conclusion is consistent with lattice QCD findings [47, 48] and some QCD effective field theory [49–52]. We also find that a moving system will reach the phase transition point at a lower temperature than a stationary system. It means that the lifetime of the moving QGP becomes longer than the static one.

The dependence of the change of phase transition temperature caused by anomalous flow on moving rapidity η at different magnetic field eB is shown in Fig. 5. Under the same dipole moving rapidity, the greater the magnetic field eB , the greater the reduction of phase transition temperature. On the other hand, under the same magnetic field eB , the faster the moving dipole, the greater the reduction of phase transition temperature.

IV. THE FREE ENERGY AND ENTROPY OF A MOVING QUARKONIUM IN A BACKGROUND MAGNETIC FIELD

The free energy of $q\bar{q}$ pair is taken as:

$$\frac{\pi}{\sqrt{\lambda}} F_{q\bar{q}} = \int_0^{z_0} \left(\sqrt{\frac{g_2(z)g_1(z)}{g_2(z) - g_{20}(z_0^{(0)})}} - \sqrt{g_2(z \rightarrow 0)} \right) dz - \int_{z_0}^{\infty} \sqrt{g_2(z \rightarrow 0)} dz \quad (25)$$

by expanding z_0 to the leading order in v_{anom} in the presence of the anomalous flow, we can get

$$z_0 \approx z_0^{(0)} + v_{\text{anom}} z_1 + O(v_{\text{anom}}^2). \quad (26)$$

Let $\tilde{z} = \frac{z}{z_0}$, and the free energy is shown as

$$\frac{\pi}{\sqrt{\lambda}} F_{q\bar{q}} = \int_0^1 \left(\sqrt{\frac{g_2(\tilde{z}z_0)g_1(\tilde{z}z_0)}{g_2(\tilde{z}z_0) - g_{20}(z_0^{(0)})}} - \sqrt{g_2(\tilde{z}z_0 \rightarrow 0)} \right) d\tilde{z}z_0 - \int_1^\infty \sqrt{g_2(\tilde{z}z_0 \rightarrow 0)} d\tilde{z}z_0, \quad (27)$$

where

$$g_2(\tilde{z}z_0) \approx g_{20}(\tilde{z}z_0^{(0)}) + (g'_{20}(\tilde{z}z_0^{(0)})\tilde{z}z_1 + g_{21}(\tilde{z}z_0^{(0)}))v_{\text{anom}}, \quad (28)$$

$$g_1(\tilde{z}z_0) \approx g_{10}(\tilde{z}z_0^{(0)}) + (g'_{10}(\tilde{z}z_0^{(0)})\tilde{z}z_1 + g_{11}(\tilde{z}z_0^{(0)}))v_{\text{anom}}. \quad (29)$$

Let $z' = \tilde{z}z_0^{(0)}$, Eq.(28) and Eq.(29) become to

$$g_2(z' \frac{z_0}{z_0^{(0)}}) \approx g_{20}(z') + (g'_{20}(z') \frac{z'_1}{z_0^{(0)}} + g_{21}(z'))v_{\text{anom}}, \quad (30)$$

$$g_1(z' \frac{z_0}{z_0^{(0)}}) \approx g_{10}(z') + (g'_{10}(z') \frac{z'_1}{z_0^{(0)}} + g_{11}(z'))v_{\text{anom}}. \quad (31)$$

After dropping the prime, we get the free energy

$$\frac{\pi}{\sqrt{\lambda}} F_{q\bar{q}} = \frac{z_0}{z_0^{(0)}} \int_0^{z_0^{(0)}} \left(\sqrt{\frac{g_2(z \frac{z_0}{z_0^{(0)}})g_1(z \frac{z_0}{z_0^{(0)}})}{g_2(z \frac{z_0}{z_0^{(0)}}) - g_{20}(z_0^{(0)})}} - \sqrt{g_2(z \rightarrow 0)} \right) dz - \frac{z_0}{z_0^{(0)}} \int_{z_0^{(0)}}^\infty \sqrt{g_2(z \rightarrow 0)} dz. \quad (32)$$

When $v_{\text{anom}} = 0$, then free energy of $q\bar{q}$ is written as

$$\frac{\pi}{\sqrt{\lambda}} F_{q\bar{q}} = \int_0^{z_0^{(0)}} \left(\sqrt{\frac{g_{20}(z)g_{10}(z)}{g_{20}(z) - g_{20}(z_0^{(0)})}} - \sqrt{g_{20}(z \rightarrow 0)} \right) dz - \int_{z_0^{(0)}}^\infty \sqrt{g_{20}(z \rightarrow 0)} dz. \quad (33)$$

The entropy of $q\bar{q}$ pair can be given as

$$S_{q\bar{q}} = -\frac{\partial F_{q\bar{q}}}{\partial T}, \quad (34)$$

when $v_{\text{anom}} = 0$, then free energy of $q\bar{q}$ is written as

$$S_{q\bar{q}}^{(0)} = -\frac{\partial F_{q\bar{q}}^{(0)}}{\partial T}. \quad (35)$$

And we also define free energy at $L = \infty$, $F_\infty = F(L \rightarrow \infty, T)$, and entropy at $L = \infty$, $S_\infty = \frac{\partial F_\infty}{\partial T}$.

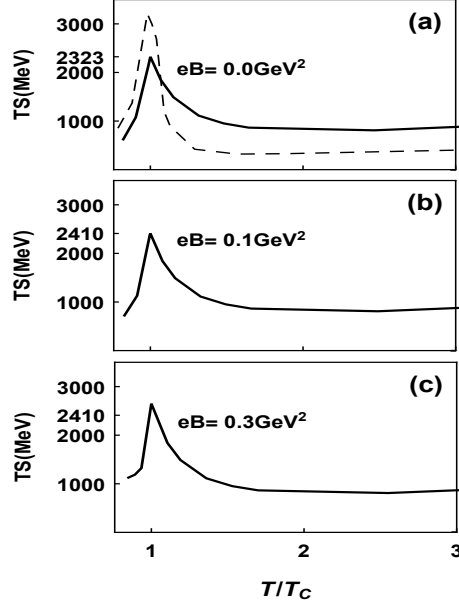


FIG. 6. The dependence of entropy (TS) on temperature (T/T_C) at different magnetic field. A comparison between our calculated results and the lattice QCD results is shown in Fig. 6(a). The solid line is our calculated results, and the dashed line are the lattice QCD results.

The lattice QCD shows the presence of an additional entropy associated at a chemical potential $\mu \rightarrow 0$ and $eB \rightarrow 0$ in the QCD plasma, and it shows a peak of entropy at the deconfinement transition [53–55] as shown in Fig. 6(a). It is found that our calculated results also show a peak of the heavy quark-antiquark entropy in the deconfinement transition and fits well with the lattice QCD theory. With the increase of magnetic field (shown in Fig. 6(b and c)), the peak value of corresponding phase transition point ($T = T_C$) increases with the magnetic field, but the change trend of TS with temperature does not change obviously. We utilize Eq.(34) to calculate the entropy of a quark-antiquark pair below the phase transition critical temperature. Above the phase transition critical temperature, the entropy of the pair equals the sum of the entropy of two single quarks, but z is on the interval $[0, z_h]$. $\lambda = 2.6$ is given in our calculation.

The dependences of entropy (TS) on magnetic field (eB) in the deconfinement phase ($T/T_C = 1.2$), Confinement-deconfinement phase transition ($T/T_C = 1$) and confinement phase ($T/T_C = 0.8$) are shown in Fig.7(a,b,c), respectively. It is found that the relationship between TS and magnetic field eB is almost the same in these three cases, that is, TS increases first to reach the maximum at $eB = 0.02 \text{ GeV}^2$, and then decreases monotonically

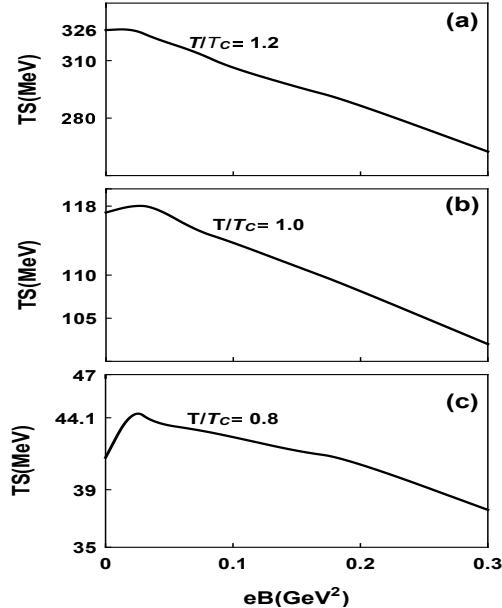


FIG. 7. The dependences of entropy (TS) on magnetic field (eB) in the deconfinement phase ($T/T_C = 1.2$) (a), Confinement-deconfinement phase transition ($T/T_C = 1$) (b) and confinement phase ($T/T_C = 0.8$)(c).

with the magnetic field. The maximum reaches 328 MeV in the deconfinement phase $T/T_C = 1.2$, and reaches only 44 MeV in the confinement phase $T/T_C = 0.8$. We also exhibit the dependences of entropy (TS) on magnetic field (eB) in the Confinement-deconfinement phase transition ($T/T_C = 1$).

V. SUMMARY AND CONCLUSIONS

It is generally believed that there will be a large magnetic field, and the confinement-deconfinement phase transition also occurs in the early stage of relativistic heavy ion non-central collision in the RHIC and LHC energy region. The strong magnetic field will produce novel anomalous transport phenomenon, which corresponds to the chiral magnetic effect and induces anomalous flow. The concept of anomalous flow is introduced to study the characteristics of the confinement-deconfinement phase transition of RHIC and LHC energy region: in the range of magnetic field (less than 0.3 GeV^2) with small chemical potential.

We use holographic correspondence to study the characteristics of the confinement-deconfinement phase transition, and establish an analytical method to quantify such in-

fluence of the anomalous flow. Such contributions stems from the modification of the bulk metric due to the chiral anomaly from the gravity side of the correspondence. Consequently, it contributes to Nambu-Goto action which determines the effective string tension. We investigate the deconfinement phase transition by analyzing the characteristics of the effective string tension with anomalous flow in a hot plasma wind to gain insight into the influence such a field can have on crucial QCD observable. The dependence of phase transition critical temperature T_C on eB at different moving rapidity η are provided, which is also one of the main results of this paper. In particular, T_C decreases with the magnetic field caused by anomalous flow. It is found that the anomalous flow would modify the characteristic of confinement-deconfinement phase transition. The deconfined phase transition manifests the characteristics of inverse magnetic catalysis, which is in qualitatively agreement with the lattice QCD findings and some QCD effective field theory. We also find that a moving system will reach the phase transition point at a lower temperature than a stationary system. It means that the lifetime of the moving QGP becomes longer than the static one.

ACKNOWLEDGMENTS

This work was supported by National Natural Science Foundation of China (Grant Nos.11875178, 11475068, 11747115).

Appendix A: Appendix:The dependence of q_c and q_{c0} in the presence of anomalous flow during phase transition

When $v_{\text{anom}} \neq 0$, in order to study the phase translation, we should make $d\sigma/dz = \dot{\sigma} = 0$ and $d^2\sigma/dz^2 = \ddot{\sigma} = 0$, and the results are given as follows:

$$(-2cMz^6 + 2cq^2z^8 + 2q^2z^6) \cosh^2 \eta + 2cz^2 - 4 - v_{\text{anom}} \sinh 2\eta[(2cz^2 - 4)Q + \dot{Q}z] = 0, \quad (\text{A1})$$

and

$$(-12cMz^5 + 16cq^2z^7 + 12q^2z^5) \cosh^2 \eta + 4cz - v_{\text{anom}} \sinh 2\eta[4czQ + (2cz^2 - 3)\dot{Q} + \ddot{Q}z] = 0, \quad (\text{A2})$$

where $\dot{Q} = \frac{dQ}{dz}$, $\ddot{Q} = \frac{d^2Q}{dz^2}$.

By solving simultaneously by Eqs.(A1) and Eqs.(A2), we study the phase transition at $T = T_C$, $z = z_c$ in the presence of anomalous flow

$$q_C^2 = \frac{2cz_c^2 - 6}{cz_c^8 \cosh^2 \eta} + v_{\text{anom}} \frac{\sinh 2\eta}{cz_c^6 \cosh^2 \eta} \left(\frac{-2cz_c^2 + 6}{z_c^2} Q - \frac{9 - 2z_c^2}{4z_c} \dot{Q} + \frac{1}{4} \ddot{Q} \right). \quad (\text{A3})$$

When $v_{\text{anom}} = 0$, which corresponds to $T = T_{C0}$, the related result of q_C is

$$q_{C0} = \sqrt{\frac{2cz_{c0}^2 - 6}{cz_c^8 \cosh^2 \eta}}. \quad (\text{A4})$$

We expand $z = z_c$ in the presence of the anomalous flow to the leading order in v_{anom} as follows:

$$z_c \approx z_{c0} + v_{\text{anom}} z_{c1} + O(v_{\text{anom}}^2). \quad (\text{A5})$$

$g_2(z_c)$ at the linear order in v_{anom} is given as

$$g_2(z_c) = g_{20}(z_c) + g_{21}(z_c)v_{\text{anom}} + O(v_{\text{anom}}^2), \quad (\text{A6})$$

from Eqs.(13) and Eqs.(A6), $g_{21}(z_c)$ can be derived as

$$g_{21}(z_c) = -\frac{h^2(z_c)}{z_c^4} Q(z_c) \sinh 2\eta, \quad (\text{A7})$$

$$g_{20}(z_c) = \frac{h^2(z_c)}{z_c^4} (f(z_c) \cosh^2 \eta - \sinh^2 \eta). \quad (\text{A8})$$

By expanding $g_{20}(z_c)$ at $z_c = z_{c0}$ of Eq.(A6), we can get:

$$\begin{aligned} g_2(z_c) &= g_{20}(z_c) + g_{21}(z_{c0})v_{\text{anom}} \\ &= g_{20}(z_{c0}) + g'_{20}(z_{c0})(z_c - z_{c0}) + g_{21}(z_{c0})v_{\text{anom}} \\ &= g_{20}(z_{c0}) + g'_{20}(z_{c0})v_{\text{anom}}z_{c1} + g_{21}(z_{c0})v_{\text{anom}} \\ &= g_{20}(z_{c0}), \end{aligned} \quad (\text{A9})$$

and

$$z_{c1} = -\frac{g_{21}(z_{c0})}{g'_{20}(z_{c0})}. \quad (\text{A10})$$

Substituting formulas (A7), (A8) and (A10) into formula (A3), we can get the result as

$$q_C^2 = \frac{2cz_{c0}^2 - 6}{cz_{c0}^8 \cosh^2 \eta} + v_{\text{anom}} G(\eta, Q, \dot{Q}, \ddot{Q}), \quad (\text{A11})$$

by defining

$$G(\eta, Q, Q', Q'') = \frac{\sinh 2\eta}{cz_{c0}^6 \cosh^2 \eta} \left(\frac{48 - 12cz_{c0}^2}{z_{c0}^3 \sinh 2\eta} + \frac{-2c0z_{c0}^2 + 6}{z_{c0}^2} Q - \frac{9 - 2z_{c0}^2}{4z_{c0}} \dot{Q} + \frac{1}{4} \ddot{Q} \right), \quad (\text{A12})$$

we can get

$$q_C^2 = q_{C0}^2 + v_{\text{anom}} G(\eta, Q, \dot{Q}, \ddot{Q}). \quad (\text{A13})$$

By expanding q_C to the leading order in v_{anom} in the presence of the anomalous flow, we can give

$$q_C = q_{C0} + v_{\text{anom}}q_{C1} + O(v_{\text{anom}}^2), \quad (\text{A14})$$

by squaring both sides of Eq.(A14) simultaneously and ignoring the higher-order term of v_{anom}^2 , we can get:

$$q_C^2 = q_{C0}^2 + 2v_{\text{anom}}q_{C0}q_{C1}. \quad (\text{A15})$$

From Eq.(A13) and Eq.(A15), q_{C1} can be given as:

$$q_{C1} = \frac{G(\eta, Q, \dot{Q}, \ddot{Q})}{2q_{C0}}, \quad (\text{A16})$$

where q_{C0} is given by Eq.(A4).

REFERENCES

-
- [1] T. Matsui and H. Satz, *Phys. Lett. B* **178**, 416 (1986).
 - [2] R. Rapp, D. Blaschke, and P. Crochet, *Prog. Part. Nucl. Phys.* **65**, 209 (2010), [arXiv:0807.2470 \[hep-ph\]](#).
 - [3] H. Satz, *J. Phys. G* **32**, R25 (2006), [arXiv:hep-ph/0512217](#).
 - [4] H. Liu, K. Rajagopal, and U. A. Wiedemann, *Phys. Rev. Lett.* **98**, 182301 (2007), [arXiv:hep-ph/0607062](#).
 - [5] S.-Q. Feng, Y.-Q. Zhao, and X. Chen, *Phys. Rev. D* **101**, 026023 (2020), [arXiv:1910.05668 \[hep-ph\]](#).
 - [6] A. V. Sadofyev and Y. Yin, *JHEP* **01**, 052 (2016), [arXiv:1510.06760 \[hep-th\]](#).
 - [7] V. Skokov, A. Y. Illarionov, and V. Toneev, *Int. J. Mod. Phys. A* **24**, 5925 (2009), [arXiv:0907.1396 \[nucl-th\]](#).
 - [8] V. Voronyuk, V. D. Toneev, W. Cassing, E. L. Bratkovskaya, V. P. Konchakovski, and S. A. Voloshin, *Phys. Rev. C* **83**, 054911 (2011), [arXiv:1103.4239 \[nucl-th\]](#).
 - [9] A. Bzdak and V. Skokov, *Phys. Lett. B* **710**, 171 (2012), [arXiv:1111.1949 \[hep-ph\]](#).
 - [10] W.-T. Deng and X.-G. Huang, *Phys. Rev. C* **85**, 044907 (2012), [arXiv:1201.5108 \[nucl-th\]](#).

- [11] Y.-J. Mo, S.-Q. Feng, and Y.-F. Shi, *Phys. Rev. C* **88**, 024901 (2013), [arXiv:1308.4289 \[hep-ph\]](#).
- [12] Y. Zhong, C.-B. Yang, X. Cai, and S.-Q. Feng, *Adv. High Energy Phys.* **2014**, 193039 (2014), [arXiv:1408.5694 \[hep-ph\]](#).
- [13] S.-Q. Feng, L. Pei, F. Sun, Y. Zhong, and Z.-B. Yin, *Chin. Phys. C* **42**, 054102 (2018), [arXiv:1609.07550 \[nucl-th\]](#).
- [14] D. E. Kharzeev, L. D. McLerran, and H. J. Warringa, *Nucl. Phys. A* **803**, 227 (2008), [arXiv:0711.0950 \[hep-ph\]](#).
- [15] D. E. Kharzeev, K. Landsteiner, A. Schmitt, and H.-U. Yee, *Lect. Notes Phys.* **871**, 1 (2013), [arXiv:1211.6245 \[hep-ph\]](#).
- [16] V. I. Zakharov, *Lect. Notes Phys.* **871**, 295 (2013), [arXiv:1210.2186 \[hep-ph\]](#).
- [17] D. E. Kharzeev, *Prog. Part. Nucl. Phys.* **75**, 133 (2014), [arXiv:1312.3348 \[hep-ph\]](#).
- [18] J. Liao, *Pramana* **84**, 901 (2015), [arXiv:1401.2500 \[hep-ph\]](#).
- [19] Y. Guo, S. Shi, S. Feng, and J. Liao, *Phys. Lett. B* **798**, 134929 (2019), [arXiv:1905.12613 \[nucl-th\]](#).
- [20] D. She, S.-Q. Feng, Y. Zhong, and Z.-B. Yin, *Eur. Phys. J. A* **54**, 48 (2018), [arXiv:1709.04662 \[hep-ph\]](#).
- [21] A. V. Sadofyev, V. I. Shevchenko, and V. I. Zakharov, *Phys. Rev. D* **83**, 105025 (2011), [arXiv:1012.1958 \[hep-th\]](#).
- [22] K. Rajagopal and A. V. Sadofyev, *JHEP* **10**, 018 (2015), [arXiv:1505.07379 \[hep-th\]](#).
- [23] O. Andreev and V. I. Zakharov, *JHEP* **04**, 100 (2007), [arXiv:hep-ph/0611304](#).
- [24] X. Chen, S.-Q. Feng, Y.-F. Shi, and Y. Zhong, *Phys. Rev. D* **97**, 066015 (2018), [arXiv:1710.00465 \[hep-ph\]](#).
- [25] H. Bohra, D. Dudal, A. Hajilou, and S. Mahapatra, *Phys. Lett. B* **801**, 135184 (2020), [arXiv:1907.01852 \[hep-th\]](#).
- [26] D. M. Rodrigues, E. Folco Capossoli, and H. Boschi-Filho, *Phys. Lett. B* **780**, 37 (2018), [arXiv:1709.09258 \[hep-th\]](#).
- [27] D. M. Rodrigues, E. Folco Capossoli, and H. Boschi-Filho, *Phys. Rev. D* **97**, 126001 (2018), [arXiv:1710.07310 \[hep-th\]](#).
- [28] D. M. Rodrigues, D. Li, E. Folco Capossoli, and H. Boschi-Filho, *Phys. Rev. D* **98**, 106007 (2018), [arXiv:1807.11822 \[hep-th\]](#).

- [29] B. McInnes, *Nucl. Phys. B* **906**, 40 (2016), [arXiv:1511.05293 \[hep-th\]](#).
- [30] U. Gürsoy, M. Jarvinen, and G. Nijs, *Phys. Rev. Lett.* **120**, 242002 (2018), [arXiv:1707.00872 \[hep-th\]](#).
- [31] U. Gürsoy, I. Iatrakis, M. Järvinen, and G. Nijs, *JHEP* **03**, 053 (2017), [arXiv:1611.06339 \[hep-th\]](#).
- [32] D. Dudal and T. G. Mertens, *Phys. Rev. D* **97**, 054035 (2018), [arXiv:1802.02805 \[hep-th\]](#).
- [33] P. Colangelo, F. Giannuzzi, and S. Nicotri, *Phys. Rev. D* **83**, 035015 (2011), [arXiv:1008.3116 \[hep-ph\]](#).
- [34] R.-G. Cai, S. He, and D. Li, *JHEP* **03**, 033 (2012), [arXiv:1201.0820 \[hep-th\]](#).
- [35] Y. Yang and P.-H. Yuan, *JHEP* **12**, 161 (2015), [arXiv:1506.05930 \[hep-th\]](#).
- [36] D. T. Son and P. Surowka, *Phys. Rev. Lett.* **103**, 191601 (2009), [arXiv:0906.5044 \[hep-th\]](#).
- [37] J. Erdmenger, M. Haack, M. Kaminski, and A. Yarom, *JHEP* **01**, 055 (2009), [arXiv:0809.2488 \[hep-th\]](#).
- [38] N. Banerjee, J. Bhattacharya, S. Bhattacharyya, S. Dutta, R. Loganayagam, and P. Surowka, *JHEP* **01**, 094 (2011), [arXiv:0809.2596 \[hep-th\]](#).
- [39] O. Andreev, *Phys. Rev. D* **73**, 107901 (2006), [arXiv:hep-th/0603170](#).
- [40] O. Andreev and V. I. Zakharov, *Phys. Rev. D* **74**, 025023 (2006), [arXiv:hep-ph/0604204](#).
- [41] O. Andreev, *Phys. Rev. D* **81**, 087901 (2010), [arXiv:1001.4414 \[hep-ph\]](#).
- [42] E. Megias and F. Pena-Benitez, *JHEP* **05**, 115 (2013), [arXiv:1304.5529 \[hep-th\]](#).
- [43] K. Tuchin, *Phys. Rev. C* **83**, 017901 (2011), [arXiv:1008.1604 \[nucl-th\]](#).
- [44] K. Marasinghe and K. Tuchin, *Phys. Rev. C* **84**, 044908 (2011), [arXiv:1103.1329 \[hep-ph\]](#).
- [45] K. Fukushima and K. Mameda, *Phys. Rev. D* **86**, 071501 (2012), [arXiv:1206.3128 \[hep-ph\]](#).
- [46] B.-X. Chen and S.-Q. Feng, *Chin. Phys. C* **44**, 024104 (2020), [arXiv:1909.10836 \[hep-ph\]](#).
- [47] G. S. Bali, F. Bruckmann, G. Endrodi, Z. Fodor, S. D. Katz, and A. Schafer, *Phys. Rev. D* **86**, 071502 (2012), [arXiv:1206.4205 \[hep-lat\]](#).
- [48] G. S. Bali, F. Bruckmann, G. Endrödi, S. D. Katz, and A. Schäfer, *JHEP* **08**, 177 (2014), [arXiv:1406.0269 \[hep-lat\]](#).
- [49] R. L. S. Farias, K. P. Gomes, G. I. Krein, and M. B. Pinto, *Phys. Rev. C* **90**, 025203 (2014), [arXiv:1404.3931 \[hep-ph\]](#).
- [50] M. Ferreira, P. Costa, O. Lourenço, T. Frederico, and C. Providência, *Phys. Rev. D* **89**, 116011 (2014), [arXiv:1404.5577 \[hep-ph\]](#).

- [51] A. Ayala, M. Loewe, A. J. Mizher, and R. Zamora, *Phys. Rev. D* **90**, 036001 (2014), [arXiv:1406.3885 \[hep-ph\]](#).
- [52] N. Mueller and J. M. Pawłowski, *Phys. Rev. D* **91**, 116010 (2015), [arXiv:1502.08011 \[hep-ph\]](#).
- [53] O. Kaczmarek, F. Karsch, P. Petreczky, and F. Zantow, *Phys. Lett. B* **543**, 41 (2002), [arXiv:hep-lat/0207002](#).
- [54] P. Petreczky and K. Petrov, *Phys. Rev. D* **70**, 054503 (2004), [arXiv:hep-lat/0405009](#).
- [55] O. Kaczmarek and F. Zantow, *PoS LAT2005*, 192 (2006), [arXiv:hep-lat/0510094](#).